Dental Materials Journal 2020; 39(6): 1080–1086

Silicon nitride ceramic for all-ceramic dental restorations

Mahmut Sertaç ÖZDOĞAN[1], Mustafa GÜNGÖRMÜŞ[2,3], Ali ÇELİK[4] and Gülsüm TOPATEŞ[5]

[1] *Department of Prosthodontics, Ankara Yıldırım Beyazıt University, Ankara, Turkey*
[2] *Department of Biomedical Engineering, Ankara Yıldırım Beyazıt University, Ankara, Turkey*
[3] *Department of Basic Sciences School of Dentistry, Ankara Yıldırım Beyazıt University, Ankara, Turkey*
[4] *Department of Metallurgical and Materials Engineering, Bilecik Şeyh Edebali University, Bilecik, Turkey*
[5] *Department of Metallurgical and Materials Engineering, Ankara Yıldırım Beyazıt University, Ankara, Turkey*
Corresponding author, Mahmut Sertaç ÖZDOĞAN; E-mail: msozdogan@ybu.edu.tr

Silicon nitride (Si_3N_4) is one of the promising ceramics for dental restoration due to providing significant benefits during the application. This study aimed to investigate the potential use of Si_3N_4 for all-ceramic dental restorations by characterizing some critical properties as color shade, mechanical resistance, shear-bond strength and radiolucency. For our study, porous Si_3N_4 ceramic was produced by partial sintering process with limited amounts of sintering additives and low temperature. A commercial ZrO_2 ceramic was prepared according to manufacturer's instructions and results were compared with Si_3N_4. Si_3N_4 is an attractive ceramic for dental applications with good mechanical properties even in porous form, it has additional advantages over the conventional ceramics used as restorative material, such as, inherent antibacterial/anti-infective activity, radiolucency, and lower hardness. It is expected that Si_3N_4 will become popular in dental applications as well.

Keywords: Bioengineering, Biomaterial(s), Crowns, Dental materials, Ceramics

INTRODUCTION

In recent years, ceramic restorations without metal infrastructure have become more popular due to their superior aesthetics and biocompatibility. The development of high toughness and high strength ceramic materials with new techniques have attracted the attention of dentists, dental technicians and patients. The increased awareness of metal-free prosthesis restorations has led to the development of many ceramic restoration systems[1-3].

Due to its good mechanical properties, ZrO_2 is widely used in medical and engineering fields[4]. Even though ZrO_2 provides many advantages in dental applications, it shows low temperature degradation (aging), which is aggravated in the presence of water. This degradation results in grain pullout, microcracking accompanying strength decreases[5]. Therefore, search for novel ceramic systems in the field of dentistry continues.

Si_3N_4 is an attractive ceramic restorative application. Due to its high wear resistance, proper fracture toughness and moderate elastic modulus, it has been adopted for biomedical applications, specifically for orthopedic joint implants[6,7]. Several studies have shown that, besides its good mechanical properties, Si_3N_4 is a biocompatible material for implant or prosthetic purposes[8,9].

Another attractive attribute of Si_3N_4 as restorative material is its inherent radiolucency. An ideal restorative material is expected to have a high enough radiopacity to be able to be distinguished from the surrounding tissues and low enough radiopacity to allow detection of voids in the material and recurrent caries[10]. The most common synthetic dental ceramic, Yttria-stabilized tetragonal zirconia polycrystalline (Y-TZP), have the same radiopacity with metals used in dentistry, such as Cr-Ni alloy and gold[11]. The low radiopacity of Si_3N_4, on the other hand, allows for both the implant and the underlying bone to be imaged using plain radiography in orthopedic applications[12].

Bacterial adhesion/colonization on restorative materials is an important factor determining the risk for secondary caries formation. One of the reasons Si_3N_4 is considered as a dental restorative/implant material is its inherent antimicrobial properties. The exact mechanism of Si_3N_4's antimicrobial activity is still being investigated but several mechanisms have been proposed. Ultra-hydrophilic and strong negative charged Si_3N_4 surfaces are easily obtainable[13]. The ultra-hydrophilicity results in a highly ordered water structure close to the surface, which acts as a physical barrier against bacteria coming into direct contact with the surface[14]. The strong negative surface charge is also thought to contribute to the antimicrobial effect by resulting in an electrostatic repulsion between the also negatively charged bacterial membrane[15]. Another mechanism that has been shown to contribute to antimicrobial behavior is formation of peroxynitrite that is toxic for several bacteria types through oxidation process[16-18].

Despite its opportune combination of properties, there is a limited number of studies on the potential of Si_3N_4 as a dental material. One of the main reasons is the improper color of Si_3N_4 ceramics for core/crown applications[19]. The color of Si_3N_4 ceramics are affected

Color figures can be viewed in the online issue, which is available at J-STAGE.
Received Apr 16, 2020: Accepted Jul 14, 2020
doi:10.4012/dmj.2020-134 JOI JST.JSTAGE/dmj/2020-134

by various factors, such as, type and oxidation state of the rare-earth additives, impurities, grain boundaries and porosity. Dense Si_3N_4 ceramics are considered too dark colored for especially restorative applications. However, lighter colors, suitable for dental applications, can be obtained when open porosity is introduced into Si_3N_4 ceramics[20].

This work aims to investigate some critical properties of Si_3N_4 for possible restorative applications. Si_3N_4 ceramic were produced *via* partial sintering, thus some amount of open porosity was formed within samples. Physical, mechanical, adhesive, optical and radiolucency properties of the produced ceramics were characterized and compared with a commercial ZrO_2 dental ceramic.

MATERIALS AND METHODS

Preparation of samples

1. Fabrication of Si_3N_4 samples

Si_3N_4 ceramics were prepared using α-Si_3N_4 powder (SN-E-10, Ube Industries, Yamaguchi, Japan) by adding 2.50 wt% Y_2O_3 (Grade C, H.C. Starck, Selb, Germany) and 2.50 wt% CeO_2 (Inframat, Manchester, CT, USA) as sintering additives. Uniaxial dry pressing was used for shaping the samples.

For three-point flexural test, bar-shaped samples were prepared according to ISO 14704:2000. For radiography and color shade measurement tests, disk-shaped samples with a diameter of 10 mm and 0.50, 1.00 and 1.50 mm thickness were prepared (n=10 for each thickness).

For shear bond strength (SBS) test, 5×5×5 mm cubic samples were prepared. All samples were sintered by pressureless sintering in a graphite furnace (FCT Anlagenbau, Germany) at 1,700°C for 1 h under N_2 atmosphere.

2. Fabrication of ZrO_2 samples

For radiography and color shade measurement tests, disk-shaped samples with a diameter of 10 mm and 0.50, 1.00 and 1.50 mm thickness were prepared (n=10 for each thickness).

For SBS test, 3×3×3 mm cubic specimens were prepared. All ZrO_2 samples were prepared from commercially available pre-sintered ZrO_2 discs (Zirking, Huge Dental, Shandong, China) using a CAD-CAM device (CAD; Dental Wings Open System, DWOS, Montréal, Canada, CAM: Yenadent D40 CAM, ZenoTec, Istanbul, Turkey). ZrO_2 specimens were sintered in a high-temperature furnace (Protherm MoS-B 150/1, Alser Teknik, Ankara, Turkey) for 2 h at 1,375°C.

Both Si_3N_4 and ZrO_2 samples were airborne-particle abraded with 50 μm Al_2O_3 particles (BEGO Korox, Bremen, Germany) applied perpendicular to the specimen surface at 0.28 MPa pressure, from 10 mm distance for 20 s. All specimens (except for Si_3N_4 bars) were polished using 800-grit silicon carbide (SiC) paper (Struers, Willich, Germany).

3. Physical and mechanical characterization of samples

Open porosity and bulk density values of samples were determined by Archimedes' displacement method according to ASTM C-20 standards[21]. Pore size distribution was measured by mercury intrusion porosimetry (MIP) (Autopore IV, Micromeritics, Norcross, GA, USA).

X-ray diffraction (XRD) was performed for phase analysis using monochromatic Cu-Kα radiation (λ=1.5406 Å) (Rigaku MiniFlex-600, Tokyo, Japan). The microstructure was investigated by scanning electron microscopy (SEM) (Hitachi SU5000, Tokyo, Japan) from the fracture surface of samples.

Mechanical characterization of samples was done according to ASTM C1161-18 standards[22]. Using ten specimens with 3×4×50 mm dimensions, three-point flexural strength and elastic modulus measurements were done. Bending load was applied using a universal testing machine (Instron 5581, Backinghamshire, UK) at a cross-head speed of 0.5 mm/min with a support span of 40 mm. Due to the porosity of Si_3N_4 samples, no grinding and polishing steps were applied for bar specimens. Hardness measurements were performed by Vickers indenter (Shimadzu HMV-G, Kyoto, Japan) at load of 98 N for 10 s.

Color shade measurement

Color shade measurements were performed between 400–700 nm with a clinical spectrophotometer (VITA Easyshade V, VITA Zahnfabrik, Bad Säckingen, Germany) with a probe tip of 5 mm. Illumination of the specimen was provided by the LED light from the periphery of the tip into the specimen surface. The display of the spectrophotometer shows the closest VITA shade in the VITA Classical shade guide from A1 to D4. The samples were photographed with Vita Classical A1-D4 Shade Guide under naturel daylight.

Shear-bond strength measurement

The SBS measurements were done on extracted caries free third molars. The protocol was approved by the Ethics Committee of the Ankara Yıldırım Beyazıt University, under the protocol number 29.05.2019/40.

Twenty caries free third molars were collected at the Tepebasi Oral and Dental Health Hospital of Ankara Yıldırım Beyazıt University, Turkey. Collected teeth were kept in 0.5% Chloramine T (Explicit Chemicals, Pune, India) at 4°C until the time of use. The teeth were cut in mesiodistal direction just above the cementoenamel junction using a Micracut 201 automated precision cutting machine with water cooling (Metkon, Bursa, Turkey) to expose a flat dentin. The exposed dentin surfaces were visually investigated to ensure the absence of residual enamel and exposure of the pulp. Teeth with residual enamel were further ground down until flat dentin surfaces were achieved. Teeth with exposed pulp were not used. The teeth were then embedded in self-curing dental acrylic (IMICRYL Cold cure, Konya, Turkey) up to a few millimeters below the sectioned surface with the aid of a plastic mold.

The prepared specimens were randomly assigned into three groups (n=10 for each group). In group 1 Si_3N_4 cubes were first treated with a silane coupling agent (Ultradent, South Jordan, UT, USA) for 2 min and then luted to dentin. In group 2 and 3 Si_3N_4 and ZrO_2 cubes were luted to dentin directly, without pretreatment with a coupling agent. Panavia Cement SA Plus (Kuraray Noritake Dental, Tokyo, Japan) was used as adhesive in all groups. Each cube was luted under 1 kg fixed pressure and light-cured for 20 s from four sides (5 s×4 sides) using an LED lamp (Linuo, Yunnan, China) with a light output of not less than 800 mW/cm^2.

The cemented specimens were subjected to thermal cycling alternating between 5°C and 55°C for 72 h using an automated thermal cycler (THE-1100, SD Mechatronik, Feldkirchen-Westerham, Germany). Following the thermal cycling, shear strength measurements were performed using a universal testing machine (Lloyd LRX, Ametek, Berwyn, PA, USA). A force parallel to the sectioned surface was applied at the base of the cubes with 1 mm/min cross-head speed until fracture. One-way ANOVA (α=0.05) was used for statistical analysis of the SBS measurements.

Radiopacity measurement

Disk shaped Si_3N_4 and ZrO_2 specimens with thickness values of 0.50, 1.00 and 1.50 mm (n=10 for each group) were prepared for radiopacity measurements. Each disk was numbered, and the thickness of each disk was determined using a digital caliper. The disks were then placed on a photostimulable phosphor (PSP) imaging plate (ScanX; Air Techniques, Melville, NY, USA). A 99% pure graduated aluminum step wedge, thickness ranging from 1 to 11 mm was also placed on the PSP imaging plate as control. Radiographs were taken using a dental X-ray unit (Villa Sistemi Medicali, Buccinasco, Italy) maintaining the X-ray beam perpendicular to the specimens at 70 peak kilovoltage (kVp), 0.32 s exposure and 7 mA current[23]. The radiographs were saved as TIFF files. The radiodensity (average pixel intensity) of the samples were determined using ImageJ software v1.52a (National Institute of Health, Bethesda, MD, USA) by selecting a region on the image and measuring the pixel intensity value. First the radiodensity of each step on the aluminum step wedge was measured. Then the intensity of each disk was measured and the thickness vs. radiodensity values were plotted for the Si_3N_4, ZrO_2 and Al specimens. Kruskal-Wallis and Tukey multiple comparison tests (α=0.05) were used for statistical analysis.

RESULTS

Densification and phase development of Si_3N_4 and ZrO_2 samples

The porosity and pore characteristics of Si_3N_4 and ZrO_2 are listed in Table 1. Partial sintering (by using limited sintering additives and lower sintering temperature) enabled formation of porous Si_3N_4. Relative densities of Si_3N_4 and ZrO_2 were measured as 84.12 and 99.23%,

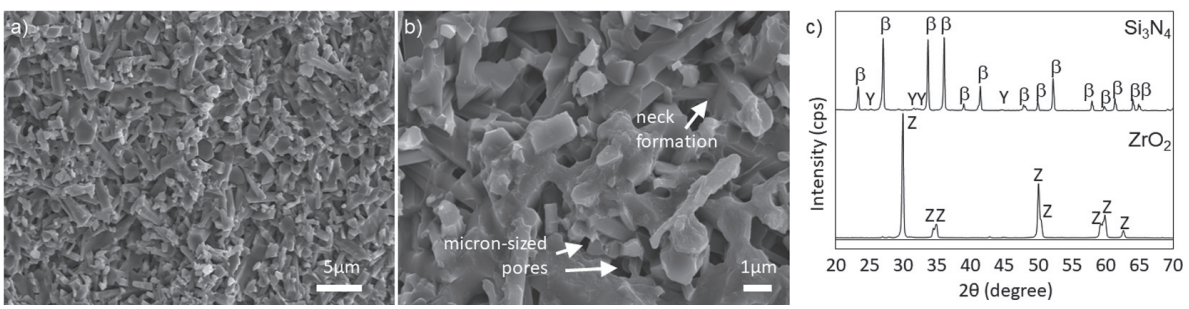

Fig. 1 SEM images of the produced Si_3N_4 ceramic under (a) 5,000× and (b) 15,000× magnification and (c) XRD patterns of Si_3N_4 and ZrO_2 (β: β-Si_3N_4, Y: Y_2SiO_4, Z: t-ZrO_2).

Table 1 Physical and mechanical properties of the Si_3N_4 and ZrO_2 ceramics used in the study. (Average±standard deviation)

Property	Si_3N_4	ZrO_2
Bulk density (g/cm^3)	2.70±0.03	6.02±0.01
Open porosity (%)	10.5±0.0	0.006±0.003
Relative density (%)	84.12±0.01	99.20±0.00
Average pore size (μm)	1.14	—
Flexural strength (MPa)	418.1±71.2	582.3±72.3
Elastic modulus (GPa)	157.5±5.4	174.5±13.5
Hardness (HV10) (GPa)	10.9±0.4	13.7±0.4

respectively. The open porosity of Si_3N_4 was 10.54% where nearly no open porosity was measured for ZrO_2.

Rod-like β-Si_3N_4 grains with various thicknesses were developed in the structure as seen in Figs. 1a and b. The presence of porosity shows that the densification was successfully controlled by partial sintering. The micron-size pore was compatible with the size of pore that was measured by MIP. Also, strong neck formation was observed (Fig. 1b), that contributes to the mechanical resistance of the ceramic.

XRD analysis showed that the produced ceramic contains β-Si_3N_4 as the major phase and Y_2SiO_4 has been formed by the reaction between Y_2O_3 and SiO_2 (the passive oxide layer of Si_3N_4) as the secondary phase (Fig. 1c). t-ZrO_2 was detected as the only phase in ZrO_2 ceramic.

Mechanical characterization of Si_3N_4 and ZrO_2 ceramics

Flexural strength, elastic modulus and hardness values of Si_3N_4 and ZrO_2 are given in Table 1. Despite the porosity of Si_3N_4, the flexural strength measured was 418 MPa due to strong neck formation between β-Si_3N_4 grains. The hardness of Si_3N_4 was measured as 10.9 GPa and for ZrO_2 13.7 GPa. If the hardness of ceramic material is high, the wear of opposing natural teeth can be observed. The lower hardness of Si_3N_4 can provide an advantage over ZrO_2 based dental ceramics.

Color shade of samples

Table 2 shows the measured L^*, a^* and b^* values of both ceramics whose thickness values are 0.5, 1.0 and 1.5 mm. L^* means the lightness coordinate of the ceramic, chromaticity coordinates of the sample are determined by a^* and b^* values. L^* ranges from 0 (absolute black) to 100 (absolute white). Positive a^* shows red when negative ($-a^*$) means green. Positive b^* indicates the yellow and negative b^* represents blue. Lower L^* values were measured for Si_3N_4 compared to ZrO_2 for all thicknesses. The photos of porous Si_3N_4 and ZrO_2 samples can be seen in Fig 2. In spite of lower L^* values of Si_3N_4, it has still whitish color that can be used for dental restorations. Also, dense Si_3N_4 sample was included to the figure for comparison. Dark coloration was obtained as the density of ceramic increased. According to Vita classical shade guide (in Fig. 2), the shades of the Si_3N_4 and ZrO_2 samples were determined as C4 and A1, respectively, for all thicknesses. Even though the shade of Si_3N_4 was in the darker range of the guide, the color is acceptable for the restorative dental applications[24,25].

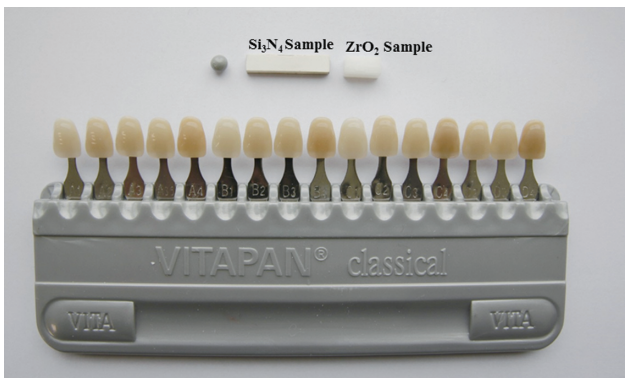

Fig. 2 Samples were photographed with Vita Classical A1-D4 Shade Guide under naturel daylight.

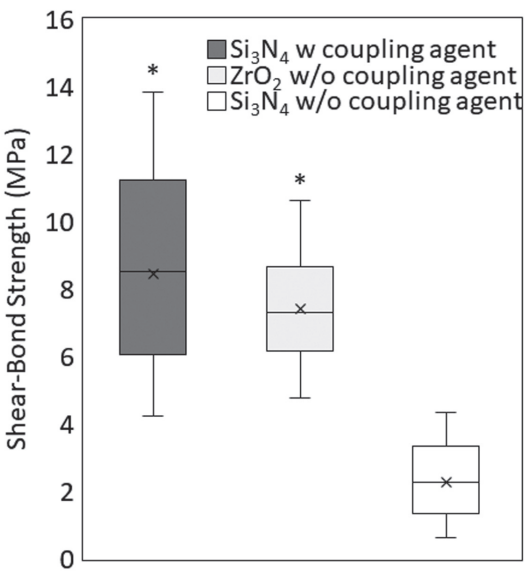

Fig. 3 Shear-bond strength values of Si_3N_4 and ZrO_2 specimens. *: no statistically significant difference (p>0.05).

Table 2 L^*, a^* and b^* values for ZrO_2 and Si_3N_4 at different thicknesses. (Average±standard deviation)

		Thickness (mm)		
		0.50	1.00	1.50
ZrO_2	L^*	98.10±2.85	97.50±2.50	95.90±1.87
	a^*	−2.20±1.36	−2.10±0.95	−2.90±1.36
	b^*	11.00±3.10	11.30±2.51	7.71±3.89
Si_3N_4	L^*	31.70±8.14	30.30±12.40	23.30±6.00
	a^*	2.46±1.98	2.51±1.99	3.62±1.51
	b^*	11.30±3.77	11.10±3.11	13.50±2.70

Table 3 Fracture pattern distribution (as Number) of samples

Sample	Adhesive failure		Cohesive failure	Mixed failure
	Dentin-cement	Ceramic-cement		
ZrO_2	4	1	1	4
Si_3N_4	1	8	—	1
Si_3N_4+silane	5	1	2	2

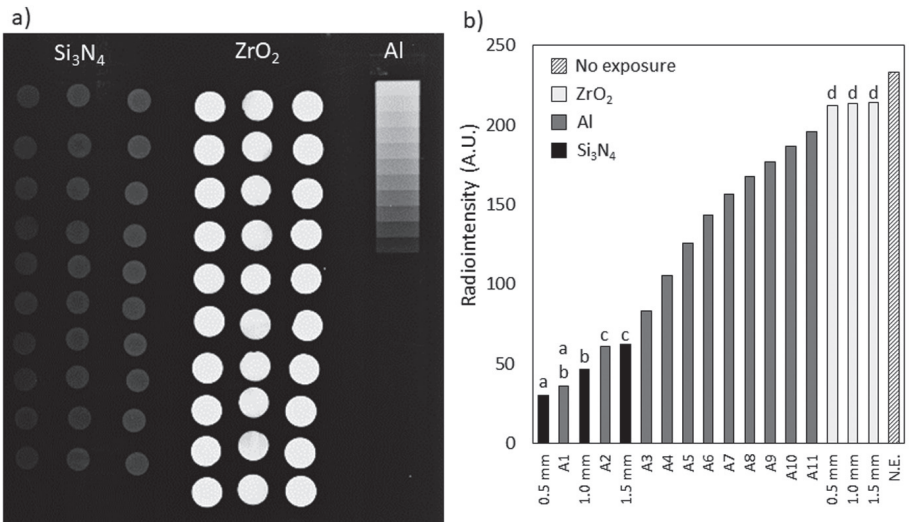

Fig. 4 (a) Radiographs and (b) radiodensity values of the Al, ZrO_2 and Si_3N_4 specimens.
a, b, c, d: no statistically significant difference (p>0.05).

Shear-bond strength evaluation

The average SBS for Si_3N_4 with coupling agent, ZrO_2 without coupling agent, and Si_3N_4 without coupling agent were 8.44±2.98 MPa, 7.42±1.92 MPa and 2.24±1.15 MPa, respectively (Fig. 3). One-way ANOVA showed a highly significant difference among the experimental groups (p<0.001). Dunnett multiple comparisons test showed no significant difference between Si_3N_4 with coupling agent and ZrO_2 without coupling agent (p=0.776). Si_3N_4 without coupling agent was significantly lower than the other groups (p<0.001).

Fracture patterns of test groups are given in Table 3. Half of the fracture patterns were adhesive failures as four adhesive failures between dentin and resin-cement, one adhesive failure between ceramic and resin-cement were observed for ZrO_2. Also, there are four mixed and one cohesive failures for this group. Again mostly adhesive failure (9/10) was seen in Si_3N_4. Si_3N_4+silane showed adhesive failure (five within dentin and cement and one within ceramic and cement).

Radiopacity evaluation

Radiographic images of the specimens and the radiointensity values are shown in Fig. 4. The ZrO_2 specimens had the highest radiointensity values. Tukey multiple comparison test showed that there was no significant difference among the ZrO_2 specimens regardless of the sample thickness, meaning at these thicknesses, ZrO_2 is almost completely opaque to X-rays. There was also no significant difference between 0.5 mm Si_3N_4 and A1, 1 mm Si_3N_4 and A1 and 1.5 mm Si_3N_4 and A2.

DISCUSSION

Densification and phase development

The main challenge in using Si_3N_4 as a dental restorative material is its gray-black color[24]. In this study, by introducing porosity into Si_3N_4 ceramics, the color was successfully tailored. The common approach to produce porous ceramic is partial sintering, where restricted sintering condition forms a uniform porous structure. In this study, porous Si_3N_4 was obtained by using lower sintering additives (5 wt%) lower sintering temperature (1,700°C) and shorter sintering duration (1 h). SEM observation of the sample shows that the microstructure was identical to that observed with partially sintered ceramics[26,27]. Fine pores were observed between the typical rod-like β-Si_3N_4 grains. These pores also indicated that sintering was finished before full consolidation took place. Instead of rounded grains, β-Si_3N_4 grains had flat sides due to lower amount of liquid content during the

sintering stage. Substantial changes observed in grains as the volume fraction of liquid (generally 2–5 vol%) is limited, a flat shape is developed in the contact regions of surrounding grains[28]. The flat tip of grains formed sharp-edged pore shape as seen in Figs. 1a and b. During the partial sintering, particles of powder compact are bonded either *via* surface diffusion or evaporation–condensation processes. A strong neck formation was observed.

Mechanical characterization

Glass ceramics, glass infiltrated ceramics, polycrystalline Al_2O_3 and ZrO_2 have been used in all ceramic dental restorations as core materials. Depending on the type of ceramic, flexural strength ranges from 150 to 1,500 MPa[29]. None of these core materials contain porosity and the flexural strength depends on the intrinsic behavior of each ceramic. Porosity is one of the flaws that results in stress concentration, and hence, reduces the strength in ceramics[30]. Since Si_3N_4 bars were tested in as-fabricated form (*i.e.*, without polishing), higher standard deviation was observed in the flexural strength measurements. Despite its porous nature, Si_3N_4 had moderate flexural strength compare to their dense counterparts. The strong neck formation between β-Si_3N_4 grains, the intertwined distribution of these grains and crack deflection potential of rod-like β-Si_3N_4 are the reasons for observed moderate strength of porous Si_3N_4[31,32]. This rod-like grains provide in-situ toughening mechanism to Si_3N_4 ceramic. Deflection of the crack along the boundaries of these specific grains, bridging of a propagating crack or pulling-out are the mechanisms to reduce the energy of crack and provide higher fracture toughness compare to other ceramics[33].

The strength of the ZrO_2 samples was also lower than the values reported in the literature. The test was conducted according to standard used for advanced ceramics. The mechanical characterization of dental materials is done according to the ISO 6872 standards, where smaller specimens are used. The probability of finding a bigger flaw or more number of defects in a larger ceramic body is higher compared to smaller size. This size difference can be the reason of observed lower strength of ZrO_2.

Hardness is another critical mechanical property in restorative materials. The lower hardness of Si_3N_4 compared to ZrO_2 is an important benefit for restorative applications. As the hardness difference between the enamel and the restorative material becomes higher, wear related problems can be experienced in the opposing natural tooth[29].

Color shade of samples

The optical properties are an important aspect of dental restorative materials. The color shade of the materials depends on many variables, such as, crystal morphology, grain size, grain boundary, porosity, *etc.* For industrial applications of Si_3N_4, the material is usually produced in a dense form. (Testing of silicon nitride ceramic bearings for total hip arthroplasty) The shade of the dense Si_3N_4 is relatively dark, gray, sometimes close to black. This limits the use of dense Si_3N_4 as a restorative material. However, due to the porous nature of the Si_3N_4 produced in this study, suitable shade (C4) for restorative use was obtained.

Shear-bond strength evaluation

A significant difference in SBS was observed between the Si_3N_4 ceramics luted to dentin with and without a silane coupling agent pre-treatment. The adhesive system used in this study, Panavia Cement SA, is an MDP monomer containing adhesive. This monomer has an M-R-X structure, where M is a metacryl group, R is the carbon chain and X is an acidic phosphate group. Acidic phosphate reacts with the metal oxides, such as ZrO_2, Al_2O_3[34]. Since Si_3N_4 is thermodynamically unstable under oxidative conditions, its surface is always covered with a 3 to 5 nm thick oxide layer[7]. Due to this oxide layer, Panavia Cement SA could not form a chemical bond with the Si_3N_4. For silica based ceramics, a silane coupling agent can be used between the ceramic and adhesive material[35]. As silane molecules are activated, methoxy (-OCH_3) groups are replaced by hydroxyl (-OH) groups and they directly react with the hydroxyl groups that exist on the surface and covalent bonds are formed *via* a condensation reaction[36]. This explains the effect of silane coupling agent on the SBS of Si_3N_4.

Radiopacity evaluation

Dentin and Al have equal radiopacity and the radiopacity of enamel is nearly twice than the radiopacity of Al with the same thickness values[37]. This study showed that radiointensity of Si_3N_4 was only slightly higher than Al, indicating that the radiopacity of Si_3N_4 is comparable to that of dentin. Lower radiointensity means partial radiolucent behavior. This provides a significant advantage for a dental material in post-operative process. The low radiopacity of Si_3N_4 will enable for both the restoration and the surrounding tissues to be imaged using plain radiography[19].

CONCLUSION

Up to now, it has been accepted that the dark-gray color of dense Si_3N_4 ceramics limits their application in restorative dentistry. This study investigated the potential use of porous Si_3N_4 for all ceramic dental restorations as a core material and results were compared with a commercial ZrO_2 ceramic. Some critical parameters were characterized to show the benefits of Si_3N_4 as a dental restorative ceramic. The color of Si_3N_4 was tailored by the porosity introduced and a color shade suitable for restorative applications was obtained. The flexural strength of Si_3N_4 was measured as 418 MPa despite the open porosity content of nearly 10.54%. The hardness of Si_3N_4 was 10.9 MPa whereas ZrO_2 had 13.7 MPa, which reduces the risk for wearing of natural teeth compared to ZrO_2. Shear bond strength test indicated that the usage of coupling agent for Si_3N_4 is essential. When coupling agent was used, Si_3N_4 had similar shear bond strength to ZrO_2. The radiolucent

behavior of Si_3N_4 shown here will enable for both the restorations and the surrounding tissues to be imaged using plain radiography. The results of this study show that with tailored manufacturing methods, Si_3N_4 can be considered as a dental restorative material.

REFERENCES

1) Duraccio D, Mussano F, Faga MG. Biomaterials for dental implants: current and future trends. J Mater Sci 2015; 50: 4779-4812.
2) Della Bona A, Pecho OE, Alessandretti R. Zirconia as a dental biomaterial. Mater 2015; 8: 4978-4991.
3) Zhang Y, Lawn BR. Novel zirconia materials in dentistry. J Dent Res 2018; 97: 140-147.
4) Guazzato M, Albakry M, Ringer SP, Swain MV. Strength, fracture toughness and microstructure of a selection of all-ceramic materials. Part II. Zirconia-based dental ceramics. Dent Mater 2004; 20: 449-456.
5) Daou EE. The zirconia ceramic: strengths and weaknesses. Open Dent J 2014; 18: 33-42.
6) McEntire B, Lakshminarayanan R, Ray D, Clarke I, Puppulin L, Pezzotti G. Silicon nitride bearings for total joint arthroplasty. Lubricants 2016; 4: 35.
7) Rahaman M, Xiao W. Silicon nitride bioceramics in healthcare. Int J Appl Ceram Technol 2018; 15: 861-872.
8) Howlett C, McCartney E, Ching W. The effect of silicon nitride ceramic on rabbit skeletal cells and tissue. An in vitro and in vivo investigation. Clin Orthop Relat Res 1989; 244: 293-304.
9) Salgueiredo E, Vila M, Silva M, Lopes M, Santos J, Costa F, *et al.* Biocompatibility evaluation of DLC-coated Si_3N_4 substrates for biomedical applications. Diam Relat Mater 2008; 17: 878-881.
10) Watts D, McCabe J. Aluminium radiopacity standards for dentistry: an international survey. J Dent 1999; 27: 73-78.
11) Pekkan G, Pekkan K, Hatipoglu MG, Tuna SH. Comparative radiopacity of ceramics and metals with human and bovine dental tissues. J Prosthet Dent 2011; 106: 109-117.
12) Ghalme S, Falak Y. Review on evolution of silicon nitride in the field of orthopedics. Current Trends in Biomedical Engineering & Biosciences (CTBEB). 2018;11:3.
13) Bock RM, McEntire BJ, Bal BS, Rahaman MN, Boffelli M, Pezzotti G. Surface modulation of silicon nitride ceramics for orthopaedic applications. Acta Biomater 2015; 26: 318-330.
14) Vogler EA. Water and the acute biological response to surfaces. J Biomater Sci Polym Ed. 1999; 10: 1015-1045.
15) Gorth DJ, Puckett S, Ercan B, Webster TJ, Rahaman M, Bal BS. Decreased bacteria activity on Si_3N_4 surfaces compared with PEEK or titanium. Int J Nanomedicine 2012; 7: 4829.
16) Ishikawa M, de Mesy Bentley KL, McEntire BJ, Bal BS, Schwarz EM, Xie C. Surface topography of silicon nitride affects antimicrobial and osseointegrative properties of tibial implants in a murine model. J Biomed Mater Res Part A 2017; 105: 3413-3421.
17) Webster TJ, Patel AA, Rahaman M, Bal BS. Anti-infective and osteointegration properties of silicon nitride, poly (ether ether ketone), and titanium implants. Acta Biomater 2012; 8: 4447-4454.
18) Pezzotti G, Bock RM, McEntire BJ, Jones E, Boffelli M, Zhu W, *et al.* Silicon nitride bioceramics induce chemically driven lysis in porphyromonas gingivalis. Langmuir 2016; 32: 3024-3035.
19) Badran Z, Struillou X, Hughes FJ, Soueidan A, Hoornaert A, Ide M. Silicon nitride (Si_3N_4) implants: the future of dental implantology? J Oral Implantol 2017; 43: 240-244.
20) Herrmann M, Goeb O. Colour of gas-pressure-sintered silicon nitride ceramics Part I. Experimental data. J Europ Ceram Soc 2001; 21: 303-314.
21) Standard Test Methods for Apparent Porosity, Water Absorption, Apparent Specific Gravity, and Bulk Density of Burned Refractory Brick and Shapes by Boiling Water, American Society for Testing and Materials; 2015.
22) Standard test method for flexural strength of advanced ceramics at ambient temperature: American Society for Testing and Materials; 2003.
23) Wadhwani C, Hess T, Faber T, Piñeyro A, Chen CS. A descriptive study of the radiographic density of implant restorative cements. J Prosthet Dent 2010; 103: 295-302.
24) Paravina RD, Powers JM, Fay RM. Dental color standards: shade tab arrangement. J Esthet Restor Dent 2001; 13: 254-263.
25) Karunaratne B, Lumby R, Lewis M. Rare-earth-doped α′-Sialon ceramics with novel optical properties. J Mater Res 1996; 11: 2790-2794.
26) Plucknett KP, Quinlan M, Garrido L, Genova L. Microstructural development in porous β-Si_3N_4 ceramics prepared with low volume RE_2O_3–MgO–(CaO) additions (RE=La, Nd, Y, Yb). Mater Sci Eng A 2008; 489: 337-350.
27) Yang J-F, Deng Z-Y, Ohji T. Fabrication and characterisation of porous silicon nitride ceramics using Yb_2O_3 as sintering additive. J Europ Ceram Soc 2003; 23: 371-378.
28) German RM. Coarsening in sintering: grain shape distribution, grain size distribution, and grain growth kinetics in solid-pore systems. Crit Rev Solid State Mater Sci 2010; 35: 263-305.
29) Ban S. Reliability and properties of core materials for all-ceramic dental restorations. Jpn Dent Sci Rev 2008; 44: 3-21.
30) Richerson DW. Modern ceramic engineering: properties, processing, and use in design: CRC press; 2005.
31) Chen W, Lv Z, Gao D, Ai X. Study on preparation and physical mechanical properties of Si_3N_4 composite ceramics. MATEC Web of Conferences 2015; 22: 05019.
32) Kawai C, Yamakawa A. Effect of porosity and microstructure on the strength of Si_3N_4: designed microstructure for high strength, high thermal shock resistance, and facile machining. J Am Ceram Soc 1997; 80: 2705-2708.
33) Bal BS, Rahaman MN. Orthopedic applications of silicon nitride ceramics. Acta Biomater 2012; 8: 2889-2898
34) Nagaoka N, Yoshihara K, Feitosa VP, Tamada Y, Irie M, Yoshida Y, *et al.* Chemical interaction mechanism of 10-MDP with zirconia. Sci Rep 2017; 7: 455-463.
35) Lung CYK, Matinlinna JP. Aspects of silane coupling agents and surface conditioning in dentistry: an overview. Dent Mater 2012; 28: 467-477.
36) Alex G. Universal adhesives: the next evolution in adhesive dentistry. Compend Contin Educ Dent 2015; 36: 15-26.
37) Ergücü Z, Türkün L, Önem E, Güneri P. Comparative radiopacity of six flowable resin composites. Oper Dent 2010; 35: 436-440.